AJNR

This information is current as of April 18, 2024.

MR Imaging Characteristics of Tuberculous Spondylitis vs Vertebral Osteomyelitis

Alison S. Smith, Meredith A. Weinstein, Akira Mizushima, Bret Coughlin, Stephen P. Hayden, Milton M. Lakin and Charles F. Lanzieri

AJNR Am J Neuroradiol 1989, 10 (3) 619-625
http://www.ajnr.org/content/10/3/619

MR Imaging Characteristics of Tuberculous Spondylitis vs Vertebral Osteomyelitis

Alison S. Smith[1]
Meredith A. Weinstein[2]
Akira Mizushima[2]
Bret Coughlin[2]
Stephen P. Hayden[3]
Milton M. Lakin[3]
Charles F. Lanzieri[2]

Retrospective evaluation was made of four patients with tuberculous spondylitis who had been studied by MR with T1- and T2-weighted images in the sagittal plane and spin-density-weighted images in the axial plane. Evaluation was made of the distribution of abnormal signals within the body and posterior elements of the vertebrae, the intervertebral disk, and the associated paraspinal and epidural areas. In two of the cases, three-level involvement was seen with noninvolvement of intervening disks; metastases were misdiagnosed. One patient had anterior/inferior erosion of the vertebral body without visualization of the disk. The last patient had the more typical MR characteristics of intervertebral disk infection. Plain film examination showed only degenerative changes in three of the four cases. MR revealed more extensive involvement than the plain films did. Involvement of the posterior element and posterior vertebral body was prominent in three of the four cases. This is a significant finding since these patients are more likely to have neurologic symptoms and require laminectomy. Follow-up examinations in two cases showed increased signal on T1-weighted images, suggesting infiltration of hemopoietic marrow with fat, as has been described for degenerative osteoarthritis. The anatomy of the microcirculation of the vertebral body is related to the patterns of vertebral osteomyelitis, and discrepancies can be seen between the findings in our cases and the MR criteria previously noted for pyogenic vertebral osteomyelitis.

The MR findings in our patients generally were more typical of neoplasm than of infection. These findings may reflect the characteristics of the tuberculous organism relative to the age-dependent pattern of vertebral microcirculation. Correct diagnosis of tuberculous spondylitis in young to middle-aged adults requires correlation of MR and clinical findings.

The appearance of vertebral osteomyelitis on MR images has been characterized as (1) confluently decreased signal intensity of the vertebral bodies and associated interspace with poor distinction between these on short TR/short TE images; (2) abnormal increased signal of the disk on long TR/long TE images with an abnormal configuration (i.e., absent intranuclear cleft); and (3) increased signal of the vertebral endplates at the abnormal disk level on long TR/long TE images [1]. In the last 30 months, four active cases of tuberculous spondylitis were treated at our institution, all of which had MR imaging. Three of the four cases did not fit the previously described MR criteria of vertebral osteomyelitis. Two of the latter were diagnosed by MR as neoplasm, and the diagnosis of tuberculosis was established at surgery. The purpose of this report is to review the MR findings of tuberculous spondylitis relative to previously described criteria and to correlate the known differences between its pathophysiology and that of pyogenic osteomyelitis.

Materials and Methods

Seven MR studies were performed in four patients with a known or final diagnosis of vertebral *Mycobacterium tuberculosis* infection. These patients had active infection at the

This article appears in the May/June 1989 issue of *AJNR* and the August 1989 issue of *AJR*.

Received March 21, 1988; accepted after revision October 11, 1988.

[1] Department of Radiology, Section of Neuroradiology, Cleveland Metropolitan General Hospital, 3395 Scranton Rd., Cleveland, OH 44109. Address reprint requests to A. S. Smith.

[2] Department of Radiology, The Cleveland Clinic Foundation, Cleveland, OH 44106.

[3] Department of Internal Medicine, The Cleveland Clinic Foundation, Cleveland, OH 44106.

***AJNR* 10:619–625, May/June 1989**
0195–6108/89/1003–0619
© American Society of Neuroradiology

time of the initial study. Two patients had a single examination. One patient had an 18-month follow-up study. One patient had 9- and 12-month interval examinations.

MR images were obtained with a 0.6-T Technicare imaging unit. Sagittal and/or coronal T1-weighted, 500/32 (TR/TE); spin-density-weighted, 2000/32; and T2-weighted, 2000/120, images were obtained, as well as axial spin-density-weighted, 1000/32, images. Most studies were performed with 5-mm slice thicknesses in sagittal and axial planes; the remaining studies used 6.5- or 7.5-mm slice thicknesses. Coronal images were 7.5 mm thick. Plain film correlation was obtained in four patients and CT correlation in one patient.

Results

The patients were 16–54 years old. The duration of symptoms was 10 weeks to 3 years at the time of initial study. Image characteristics are listed in Table 1. Two of the four patients with tuberculous spondylitis (cases 1 and 2) had involvement of three consecutive vertebral body levels (Figs. 1 and 2). The abnormal vertebrae in these patients had decreased signal on short TR/TE images with more apparent increased signal on long TR/TE images. There was no abnormal signal of the disk on long TR/TE images, but the posterior aspect of the vertebral body was prominently involved in five of six of these vertebrae with pedicle involvement at four of six levels. Plain films in case 1 showed only degenerative changes. Plain films in case 2 showed a large paraspinal mass without obvious vertebral involvement. Case 3 had anterior/inferior erosions of the L1 vertebral body and associated sclerotic changes. Long TR/TE images in case 3 indicated involvement of the entire L1 body and superior L2 endplate, while short TR/TE images basically reflected the area of plain film abnormality. The L1 disk was not identified (Fig. 3). Case 4 shows decreased signal of the endplates at the L1–L2 level with poor differentiation of the L1 disk from the associated endplates on the short TR/TE images. There was an abnormal configuration of the L1 disk and abnormal signal of the disk and endplates on the long TR/TE images (Fig. 4). Plain films showed degenerative changes at the interspace. Interspace narrowing was notable in cases 3 and 4 but not prominent in cases 1 and 2. Follow-up examinations in case 1 at 9 and 12 months showed increased signal on short TR/TE images where previous abnormality was present on long TR/TE images (Fig. 1). The long TR/TE images were normal. Follow-up examination in case 3 at 18 months showed similar but less marked changes in the short TR/TE study. Mildly increased signal was present at the endplates on the long TR/TE examination.

Discussion

Although the number of cases of pulmonary tuberculosis has markedly decreased, the incidence of bone and joint tuberculosis has not changed in the last decade [2]. Indeed, none of our patients had evidence of pulmonary tuberculosis on chest radiographs. This correlates with autopsy series in which 80% of the subjects with vertebral tuberculosis had no documented source, leading some to suggest a relationship to the primary complex [3] rather than secondary infection from another active site in the body [4–6]. Although a disease of children in developing countries, North American tuberculous spondylitis is most prevalent in adults with a mean age of 41–44 years [2, 7]. In our series (mean age, 32 years), there were one adolescent and three adults.

Classically, spinal tuberculosis is thought to begin in the anterior/inferior portion of the vertebral body [6, 7]. Spread of infection can occur beneath the longitudinal ligaments involving the adjacent vertebral bodies. Disk-space narrowing occurs secondarily and therefore usually is limited relative to

TABLE 1: MR Abnormalities in Active Tuberculous Spondylitis

Case No.	Involvement	Signal Intensity		Disk Signal	Interspace	Paraspinal Mass	Epidural Extension
		T1WI	T2WI				
1	T8: entire body and pedicles	Decreased	Increased	T7–T10: normal intensity	T8–T9: slightly narrowed	Large, lateral: T7–T11	Present
	T9: posterior one-third, body and pedicles	Decreased	Increased		T9–T10: normal		
	T10: posterior one-third, body and pedicles	Decreased	Increased		T10–T11: normal		
2	T6: posterior one-third, body	Isointense	Increased	T5–T8: normal intensity	Normal	Large, lateral: T6–T9	Present
	T7: posterior two-thirds and pedicles	Decreased	Increased				
	T8: posterior one-third and pedicles	Decreased	Increased				
3	L1: anterior/inferior body	Slightly increased	Slightly increased	L1 not visualized	L1–L2: narrowed	Absent	Absent
	L2: anterior/superior body	Slightly increased	Slightly increased				
4	L1: inferior endplate	Decreased	Increased	L1: increased; T2WI: loss of intranuclear cleft	L1–L2: moderately narrowed	Large, bilateral: L1–L5	Absent
	L2: superior endplate	Decreased	Increased				

Note.—T1WI = T1-weighted images; T2WI = T2-weighted images.

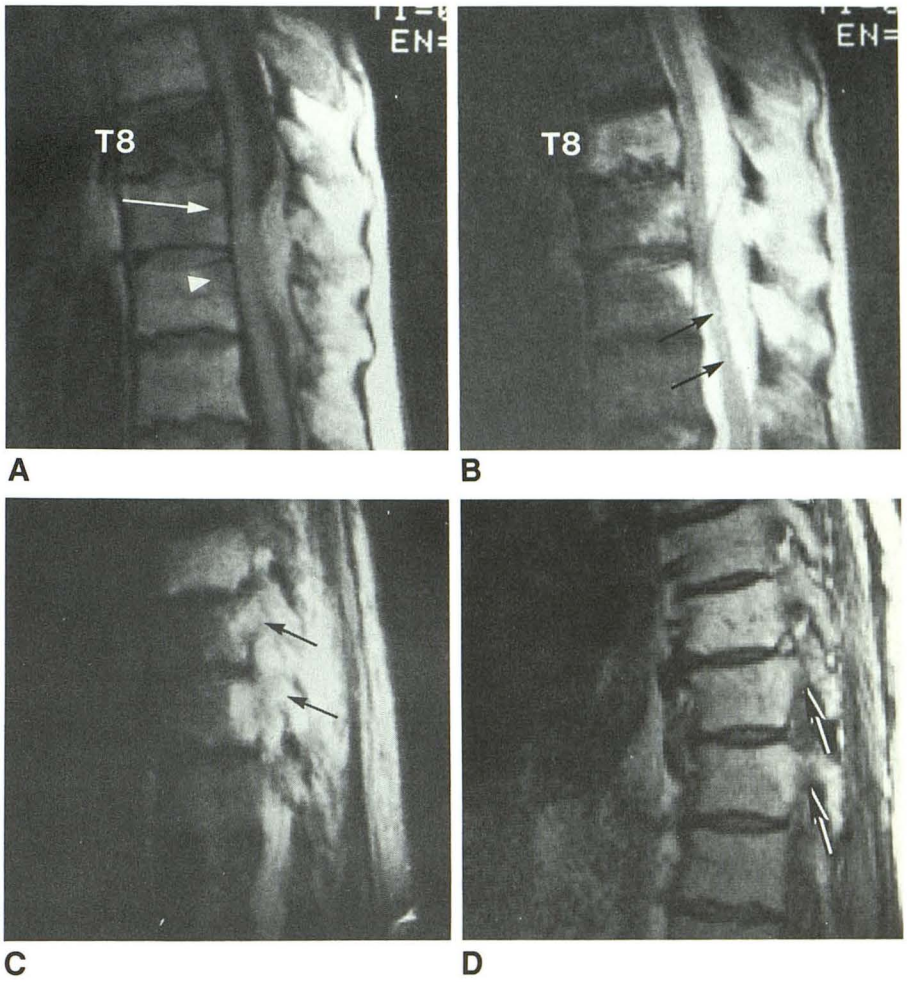

Fig. 1.—Case 1: 54-year-old woman with 3-year history of intermittent thoracolumbar pain, fever, and weight loss who was found to have tuberculosis at thoracic decompressive laminectomy.

***A*, MR image, 500/32. Hypointensity is seen in T8, T9 (*arrow*), and T10 (*arrowhead*) vertebral bodies. Posterior epidural abscess deviates cord anteriorly.**

***B*, Long TR/TE image, 3000/120, better defines location of abnormal signal within posterior aspect of T9 and T10 vertebral bodies and entire T8 vertebral body. Increased signal within associated area of spinal cord may be secondary to myelitis (*arrows*). Note.—No increased signal from disks.**

***C*, Parasagittal image, 3000/120, shows abnormally increased signal involving pedicles of T8 and T9 (*arrows*).**

***D*, 9-month follow-up examination, 500/32, shows increased signal intensity at areas of abnormality of T8–T10 vertebral bodies and pedicles of T9 and T10 (*arrows*).**

the degree of bone destruction. Destruction of the bone allows herniation of the disk material into the affected body [5, 7]. A lack of proteolytic enzymes in the *Mycobacterium* as compared with pyogenic infection has been proposed as the cause of relative preservation of the intervertebral disk [4], which has been found totally sequestered within involved vertebrae [7]. Noninvolvement of the disk on pathologic examination has been reported more often in the nonwhite population [4, 8]. Obviously, if uninvolved, the disk will not increase in signal on T2-weighted images, a uniform finding in descriptions of pyogenic infection [1]. In only one of the four cases was there increased signal intensity of the disk (Fig. 4). However, the interspace in case 3 was still clearly abnormal. Perhaps the disk was destroyed and not identified at all in this 16-year-old due to the differences in pathophysiology and vertebral microvascular circulation in adults and children, as is discussed later in this article. In addition to vertebral spondylitis, increased signal of vertebral endplates on T2-weighted images is found in the inflammatory stage of osteoarthritis. Distinction has been made between the two on the basis of lack of associated abnormal disk signal on the same images [9]. However, since tuberculosis can have similar characteristics, these findings must be viewed carefully relative to the appropriate clinical setting.

Only one of our patients (case 4) had the typical appearance of involved endplates adjacent to an abnormal intervertebral disk. Involvement of the posterior vertebral body and posterior elements was prominent in cases 1 and 2. Recognition of posterior element involvement is important in tuberculosis, since successful therapy requires laminectomy in addition to chemotherapy, and these patients are more likely to have neurologic symptoms [8]. Posterior element abnormalities with or without involvement of the vertebral body make differentiation of infection from tumor very difficult. This is especially true when they are combined with relative preservation of the disk space, a well-established criterion for the presence of neoplasm rather than infection [10]. Pedicle and posterior element involvement as well as subligamentous spread have been reported more frequently in nonwhite tuberculous patients [4, 8]. The multiplicity of vertebral body involvement in tuberculous spondylitis patients also contributes to the confusion with metastatic disease. Half of our patients had involvement of three vertebral bodies, which correlates with data from clinical [4, 11, 12] and autopsy series [3], where 50–64% of cases have three or more bodies involved. Single vertebral body involvement by tuberculosis without involvement of the disk has been recognized [4, 6, 8, 10] and like pyogenic infection seems to have an association

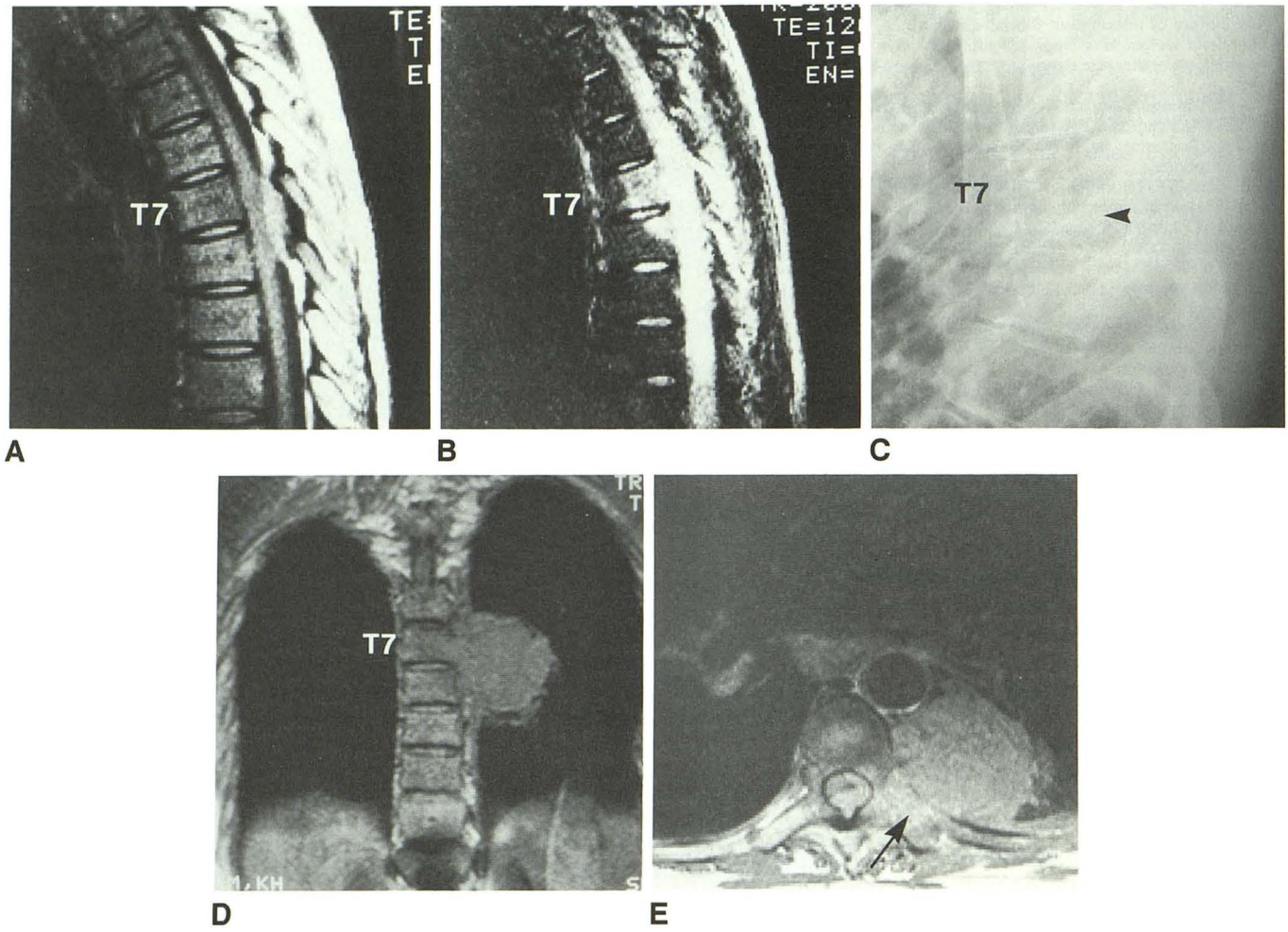

Fig. 2.—Case 2: 38-year-old woman after 10 weeks of left back and chest pain, made worse by lying on left side. Diagnosis of tuberculosis was established at laminectomy and thoracotomy.

***A*, MR image, 500/32. Posterior epidural mass is present posterior to T7 and T8, as well as decreased signal of posterior T7 body.**

***B*, Long TR/long TE image, 2000/120, better shows abnormal signal involving posterior T7 and T8. Involvement of T6 and more extensive involvement of T8 bodies were present on more lateral image.**

***C*, Lateral plain film retrospectively may show some erosion at posterior cortex of T7 vertebral body (*arrowhead*).**

***D*, Coronal image, 500/32, shows loss of lateral cortex of T7 with decreased signal of T7 and lateral T8 vertebral bodies. Large paraspinal mass and preservation of disk spaces mimic neoplasm.**

***E*, MR image, 1000/32. Epidural abscess at level of T7 compresses cord to right. There is involvement of left pedicle, transverse process (*arrow*), and T7 rib and paraspinal space.**

with osteopenia [13, 14]. It is unclear whether the involvement of multiple vertebral bodies is due to the hematogenous, subligamentous, paraspinal, or subarachnoid spread of disease, although the first possibility seems most likely.

Review of vertebral microcirculation may explain the multivertebral involvement and differences between adult and childhood spondylitis, and allow speculation about posterior body involvement in adult tuberculosis. The majority of blood in the paired segmental arteries of each vertebral body terminates in branches to the posterior elements, paraspinal musculature, and spinal branch (Fig. 5A). The spinal branch courses into the neural foramen and beneath the posterior longitudinal ligament (Fig. 5B). Anastomoses from spinal branches of the levels above and below coalesce before entering the basivertebral foramen as the nutrient equatorial artery. The nutrient equatorial artery supplies most of the vertebral body and has most of its branches posteriorly. Much smaller branches from the segmental arteries form a horseshoe-shaped anastomosis around the vertebral body, which branches to superior and inferior poles of the body. In the anatomic literature, the upper and lower ends of the vertebral body adjacent to the epiphyseal ring are termed the "metaphyses," reflecting their physiologic and embryologic origins [15]. Branch arteries have been demonstrated between the superior and inferior metaphyseal anastomosal arteries, as well as anastomoses that course in the adventitia of the intervertebral disk to join the metaphyseal anastomosing arteries of adjacent vertebrae (intermetaphyseal artery) [15, 16]. In childhood, anastomoses connect the equatorial and metaphyseal arteries. These anastomoses atrophy by age 15 and peripheral periosteal arteries develop (Fig. 5C) [15]. Redevelopment of the anastomoses between the intraosseous

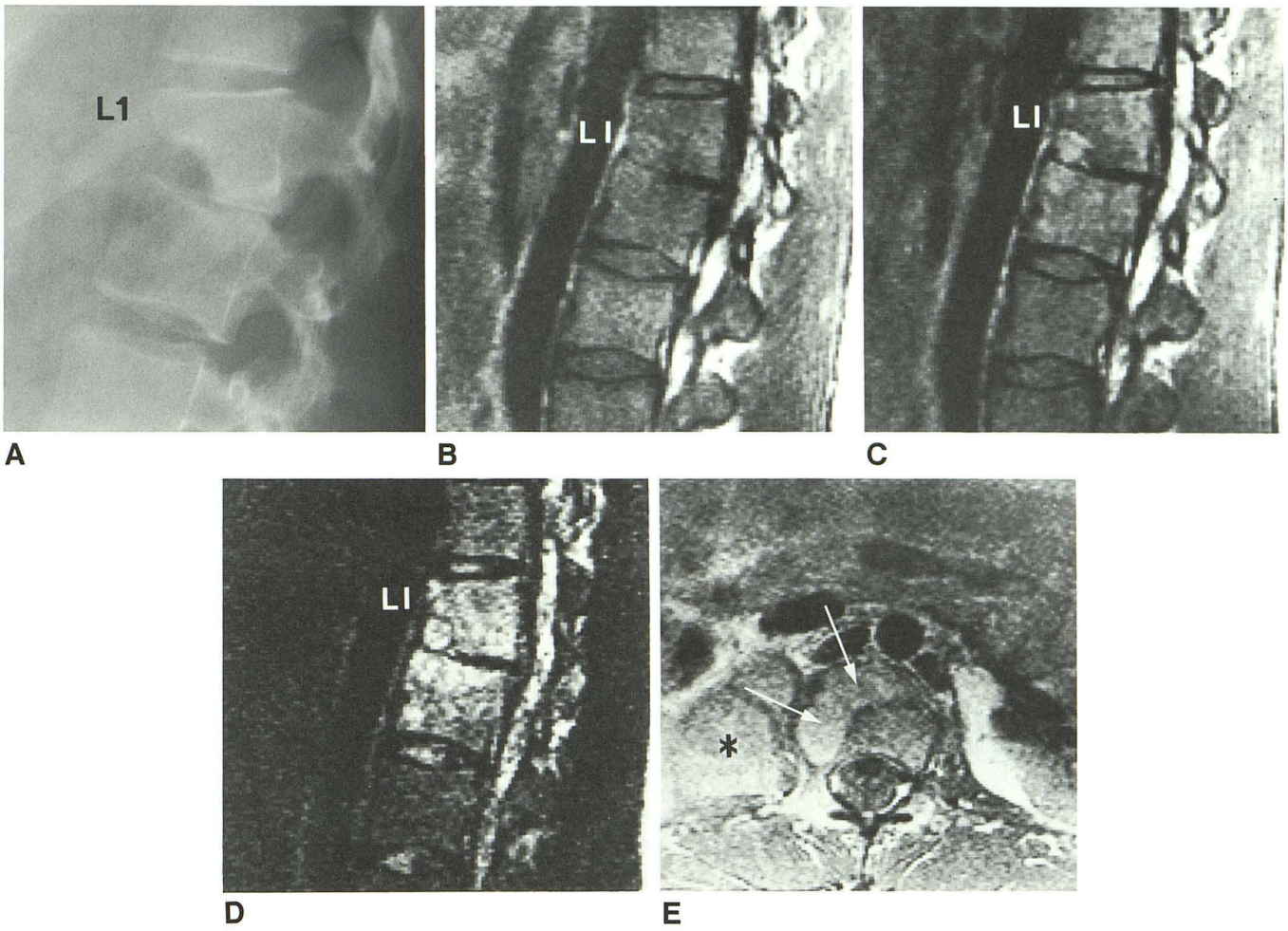

Fig. 3.—Case 3: 16-year-old boy with intermittent low-back pain for 2 years.
***A*, Plain film shows gibbus deformity with erosion of anterior/inferior aspect of L1 and lucency of anterior/superior aspect of L2 vertebral body.**
***B* and *C*, Parasagittal images, 500/32 (*B*) and 2000/32 (*C*). L1 intervertebral disk cannot be identified on either sequence. Isointense to hyperintense "kissing" lesions are seen in area of plain film abnormality.**
***D*, Long TR/TE image, 2000/120, shows much more extensive involvement of L1 and L2 vertebral bodies.**
***E*, MR image, 2000/120. Distribution of granulomatous tissue (*arrows*) at inferior endplate of L1 follows pattern of metaphyseal anastomosing artery circulation. Paraspinal mass is seen to the right (*asterisk*).**

arteries and proliferation of peripheral periosteal arteries in the elderly and in osteopenic collapse have been proposed [14–16]. It is known that bone infarction must accompany the presence of pyogenic bacteria to allow osteomyelitis to develop [5, 15]. The presence of multiple anastomoses of the interosseous arteries in children means that a septic embolus will result in only a small infarct to act as a nidus of infection. In the adult, where branches of the equatorial and metaphyseal arteries are end arteries, a larger area of infarct will occur. Retrograde infarction of the metaphyseal arteries can extend circumferentially through the metaphyseal anastomosing artery [15]. This pattern is reflected in the peripheral arcuate abnormality, mirroring the distribution of the metaphyseal anastomosing artery in Figure 3E. Extension of infection to the opposite metaphysis and the metaphysis of the adjacent vertebrae occurs through the intermetaphyseal arteries without effect on the equator of the body. The intermetaphyseal arteries are probably the route of transdiskal metaphyseal spread characteristic of pyogenic vertebral osteomyelitis in adults [16]. A concurrent diskitis that occurs at all ages, therefore, is the more prominent finding in children, while the radiologic signs of vertebral involvement predominate in adults [15]. Although both pyogenic and mycobacterial infection can be found in any distribution in the vertebral body, it is interesting to speculate that in the adult, the aerophilic mycobacteria require the higher flow of the posterior equatorial artery for sufficient oxygen concentration to survive. Although this article reports only two cases with a posterior "equatorial" distribution of tuberculous infection, *Mycobacterium tuberculosis* was the organism in nine of 19 cases with single-body involvement associated with osteopenia and vertebral fracture [13, 14]. The theory can be expanded to

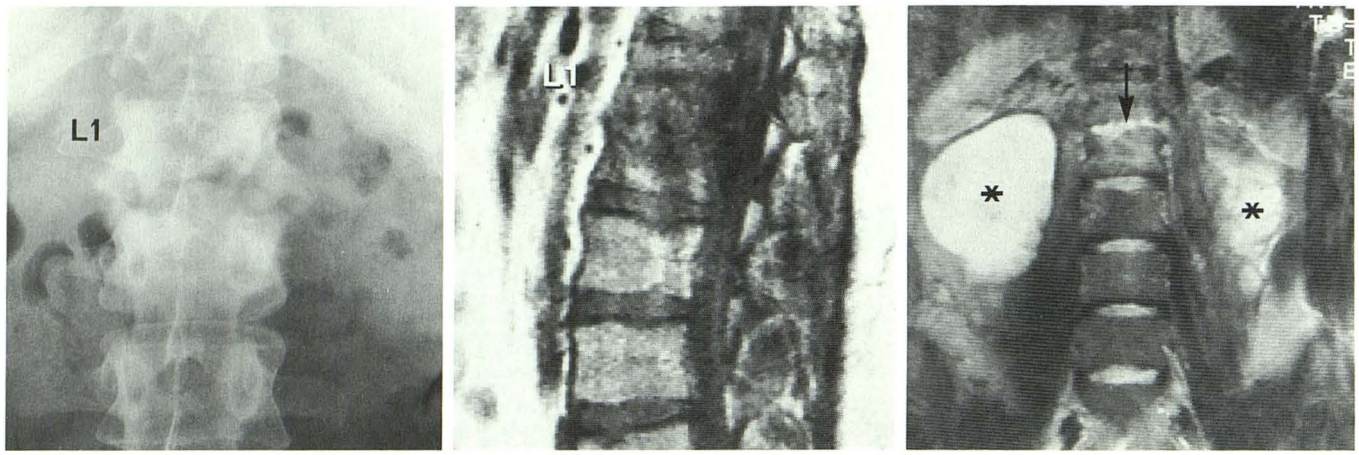

Fig. 4.—Case 4: 23-year-old man with 2-year history of intermittent low-back pain had surgery for presumed appendicitis when large right psoas abscess containing *Mycobacterium* was drained. Six months later, after 1 month of antituberculosis chemotherapy, the patient had progressive flank and back pain.

***A*, Plain film shows moderate hypertrophic, sclerotic changes at L1–L2 endplates.**

***B*, MR image, 500/32, shows decreased signal involving endplates, which cannot be distinguished from intervertebral disk at L1–L2.**

***C*, MR image, 2000/120. Abnormally increased signal is present at L1 disk with loss of intranuclear cleft (*arrow*). Large, bilateral paraspinal abscesses are seen (*asterisks*).**

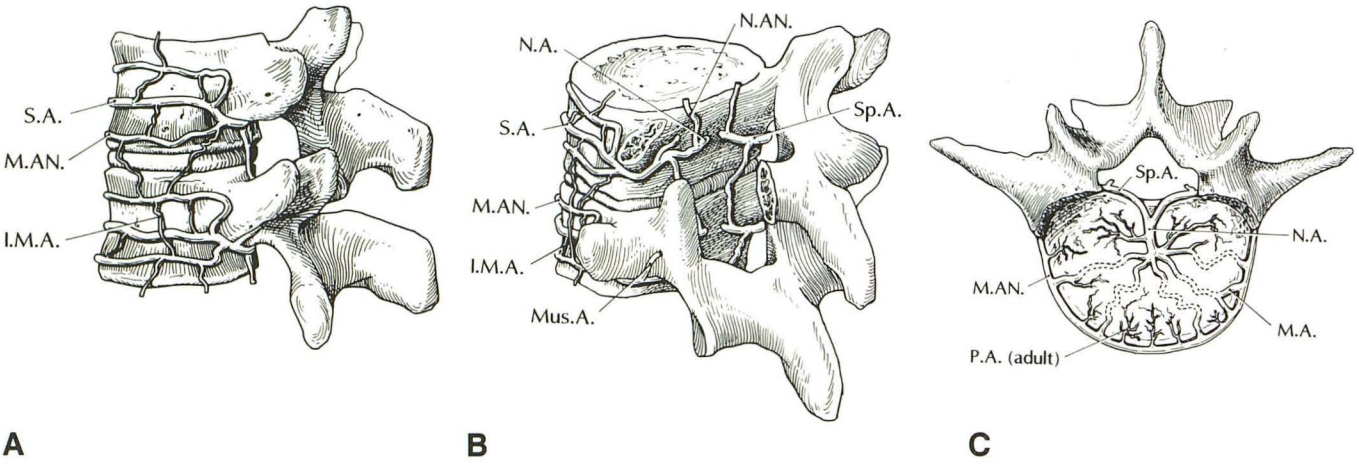

Fig. 5.—Microcirculation of vertebral bodies. (See text for description.)

***A*, Lateral view.**

***B*, Posterior oblique view with resected pedicle and lamina.**

***C*, Composite representation of cutaway surface of vertebral body.**

S.A. = segmental artery; M.AN. = metaphyseal anastomosing artery; I.M.A. = intermetaphyseal anastomosis; Sp.A. = spinal artery; N.A. = nutrient artery; N.AN. = nutrient anastomosing artery; Mus.A. = muscular artery; M.A. = metaphyseal artery; P.A. = periosteal artery.

account for the metaphyseal location of tuberculous infection that originates in childhood, when anastomoses remain between the interosseous arteries. The higher-flow equatorial circulation may flush the organisms into the metaphyseal distribution (Fig. 3E).

Our patients had moderate- to large-sized paraspinal masses, relatively out of proportion to the amount of bone destruction and interspace involvement typical of *Mycobacterium tuberculosis* [6]. The reported incidence of paraspinal masses is 55–96% [2, 3, 7, 12, 13]; the masses are characterized by a thick, irregular rim enhancement on CT [12]. The paraspinal masses in our series had no distinguishing features on the MR sequences used. However, gadolinium-DTPA has been shown to be useful in MR in delineating communications between the vertebral and paravertebral components of tuberculous spondylitis [17]. The size of the paraspinal masses has been noted to be generally larger in tuberculosis than in pyogenic infections [18]. Tumor is obviously a differential point when a paraspinal mass associated with bone destruction is present. Other potential mimics of tuberculosis on MR are actinomycosis, which spares the disk space while spreading in a subligamentous fashion, and hydatid disease, which can result in bone destruction, disk-space preservation, and paraspinal mass with or without calcification [4]. When present, calcifications in paraspinal masses seen on plain films or CT scans may suggest the diagnosis of tuberculosis.

The duration of symptoms of vertebral osteomyelitis can give clues to the presence of pyogenic vs tuberculous infec-

tion. Tuberculosis is well known for its insidious onset, with symptoms ranging from months to 2 or 3 years [2, 6, 7, 13], as exemplified by our series. The more indolent course of tuberculosis probably explains the paucity of destructive changes and the hypertrophic, regenerative attempts at healing on plain films. Pyogenic infections tend to have symptoms for days to months [18]. Although not helpful in a specific case, pyogenic vertebral osteomyelitis has a later peak occurrence; that is, in the sixth to seventh decade, than does tuberculosis [19, 20]. Tuberculosis shows definite geographic differences in the age group affected. However, as alluded to earlier, in the developed countries of the world, over half the patients are young to middle-aged adults [3, 4, 6]. Increased signal on short TR/TE images of previously involved areas of the spine was seen in the two patients who had follow-up MR. As seems to be the case in degenerative disk disease, the inflammatory process or relative ischemia within the vertebral bodies may stimulate increased conversion of hemopoietic marrow to yellow (fatty) marrow, resulting in this finding (Fig. 1D) [9].

In summary, in this small series of patients with vertebral tuberculous spondylitis, the majority of the patients exhibited MR findings more typical of neoplasm than those that have been characterized for infection. Specifically, there was a predilection for noninvolvement or lack of abnormal signal of the intervertebral disk space, involvement of posterior vertebral bodies and posterior elements rather than endplates, involvement of three vertebral bodies, and the presence of large paraspinal soft-tissue masses. These findings may relate to characteristics of the tuberculous organism relative to the age-dependent pattern of vertebral microcirculation. Differentiation from neoplastic involvement may be impossible on the basis of MR images alone. However, the constellation of the MR findings along with a long history of symptoms in a young to middle-aged adult may suggest the presence of tuberculous infection.

ACKNOWLEDGMENTS

We thank Paul M. Duchesneau, Scott A. Rosenbloom, and John J. Wasenko for assistance with this work.

REFERENCES

1. Modic MT, Feiglin DH, Piraino DW, et al. Vertebral osteomyelitis: assessment using MR. *Radiology* **1985**;157:157–166
2. Shivaram U, Wollschlager C, Khan F, Khan A. Spinal tuberculosis revisited. *South Med J* **1985**;78:681–684
3. Auerbach O, Stemmerman MG. The roentgen interpretation of the pathology in Pott's disease. *AJR* **1944**;52(1):57–63
4. Chapman M, Murray RO, Stoker DJ. Tuberculosis of the bones and joints. *Semin Roentgenol* **1979**;14(4):266–282
5. Kahn DS, Pritzker KPH. Pathophysiology of bone infection. *Clin Orthop* **1973**;96:12–19
6. Resnick D, Niwayama G. Osteomyelitis, septic arthritis and soft tissue infection. In: Resnick D, Niwayama G, eds. *Diagnosis of bone and joint disorders with emphasis on articular abnormalities*. Philadelphia: Saunders, **1981**:2141–2173
7. Weaver P, Lifeso RM. The radiological diagnosis of tuberculosis of the adult spine. *Skeletal Radiol* **1984**;12(3):178–186
8. Naim-Ur-Rahman. Atypical forms of spinal tuberculosis. *J Bone Joint Surg [Br]* **1980**;62-B:162–165
9. DeRoos A, Kressel H, Spritzer C, Dalinka M. MR imaging of marrow changes adjacent to endplates in degenerative lumbar disk disease. *AJR* **1987**;149:531–534
10. Norman A, Kambolis CP. Tumors of the spine and their relationship to the intervertebral disk. *AJR* **1964**;92(6):1270–1274
11. Raininko RK, Aho AJ, Laine MO. Computed tomography in spondylitis. *Acta Orthop Scand* **1984**;56:372–377
12. Whelan MA, Naidich DP, Post JD, Chase NE. Computed tomography of spinal tuberculosis. *J Comput Assist Tomogr* **1983**;7(1):25–30
13. LaBerge JM, Brant-Zawadzki M. Evaluation of Pott's disease with computer tomography. *Neuroradiology* **1984**;26:429–434
14. McHenry MC, Duchesneau PM, Keys TF, et al. Vertebral osteomyelitis presenting as spinal compression fracture: six patients with underlying osteoporosis. *Arch Intern Med* **1988**;148:417–423
15. Ratcliffe JF. Anatomic basis for the pathogenesis and radiologic features of vertebral osteomyelitis and its differentiation from childhood discitis. *Acta Radiol [Diagn]* (Stockh) **1985**;26(2):137–143
16. Wiley AM, Trueta J. The vascular anatomy of the spine and its relationship to pyogenic vertebral osteomyelitis. *J Bone Joint Surg [Br]* **1959**;41-B:769–809
17. DeRoos A, van Persijn van Meerten EL, Bloem JL, Bluemm RG. MRI of tuberculous spondylitis. *AJR* **1986**;146:79–82
18. Whelan MA, Schonfeld S, Post JD, et al. Computed tomography of nontuberculous spinal infection. *J Comput Assist Tomogr* **1985**;9(2):280–287
19. Waldvogel FA, Vasey H. Osteomyelitis: the past decade. *N Engl J Med* **1980**;303:360–370
20. Griffiths HEP, Jones DM. Pyogenic infection of the spine. *J Bone Joint Surg [Br]* **1971**;53-B:383–391